

Relationship between spinons and magnetic fields in a fractionalized state

Yu Zhang¹, Hengdi Zhao², Tristan R. Cao¹, Rahul Nandkishore^{1,3}, and Gang Cao^{1,4*}

¹*Department of Physics, University of Colorado at Boulder, Boulder, CO 80309, USA*

²*Materials Science Division, Argonne National Laboratory, Lemont, IL 60439, USA*

³*Center for Theory of Quantum Matter, University of Colorado at Boulder, Boulder, CO 80309, USA*

⁴*Center for Experiments on Quantum Materials, University of Colorado at Boulder, Boulder, CO 80309, USA*

The $4d$ -electron trimer lattice $\text{Ba}_4\text{Nb}_{1-x}\text{Ru}_{3+x}\text{O}_{12}$ features a universal heavy spinon Fermi surface that underpins both a quantum spin liquid (QSL) and an adjacent heavy-fermion strange metal (HFSM), depending on Nb content; the itinerant spinons as heat carriers render the charge-insulating QSL a much better thermal conductor than the HFSM [1]. Here we report that application of a magnetic field up to 14 T surprisingly breaks the signature temperature-linearity of the heat capacity of both phases below 150 mK, inducing a rapid rise in the heat capacity by as much as 5000%, whereas the AC magnetic susceptibility and the electrical resistivity show little response up to 14 T in the same milli-Kelvin temperature range. Furthermore, the magnetic field readily suppresses the thermal conductivity, and more strongly with decreasing temperature below 4 K by up to 40%. All these complex thermal phenomena indicate a powerful simplifying principle: Application of a magnetic field adversely weakens the itinerancy of spinons and eventually destroys it with decreasing temperature, leading to an unprecedented quantum state featuring the astonishing rise in the heat capacity, thus entropy in the most unlikely circumstances of milli-Kelvin temperatures and strong magnetic fields. We present and discuss possible explanations.

*Corresponding author: gang.cao@colorado.edu

It has recently been discovered that the trimer lattice $\text{Ba}_4\text{Nb}_{1-x}\text{Ru}_{3+x}\text{O}_{12}$ ($|x| < 0.20$) encompasses a coexistence of both quantum spin liquid (QSL) physics, strong electron correlations tunable across a metal-to-insulator transition, and a heavy-fermion strange metal (HFSM), as illustrated in **Fig.1a** [1]. The most striking feature shared by the entire $\text{Ba}_4\text{Nb}_{1-x}\text{Ru}_{3+x}\text{O}_{12}$ series is the persistent linearity in low-temperature heat capacity C and thermal conductivity κ , extraordinarily large Sommerfeld coefficient γ and exchange energy θ_{CW} as well as the absence of magnetic order down to 50 mK, independent of the ground state type (**Fig1.a**). Moreover, the charge-insulating QSL is a much better thermal conductor than the HFSM, and this is best explained by a charge and spin separation [1]. At the heart of the trimer lattice is a conjectured perpetual heavy Fermi surface of charge-neutral spinons that provides a unified framework for describing the novel phenomena observed throughout the entire series [1]. The discovery constitutes a breakthrough in the search of QSL that has been a focus of intense research over decades because of its wave-function entanglement and exotic excitations [e.g., 2-8].

Our most recent investigation of the trimer lattice $\text{Ba}_4\text{Nb}_{1-x}\text{Ru}_{3+x}\text{O}_{12}$ ($|x| < 0.20$; the sign of x can be either positive or negative) further reveals a seemingly enigmatic, yet extraordinarily intriguing relationship between spinons and applied magnetic fields at low temperatures T , which until now has not been explored. In essence, the magnetic field H (up to 14 T) unexpectedly breaks the signature linearity of the heat capacity C by inducing a rapid rise in C near an onset temperature $T_s = 150$ mK for both the QSL and HFSM. As a result, C is drastically increased by as much as 5000% at 50 mK. Remarkably, the H -enhanced C or ΔC is independent of the orientation of H , indicating the absence of orbital degrees of freedom. Furthermore, no corresponding responses are discerned in both the AC magnetic susceptibility χ' of the QSL and electrical resistivity ρ of the HFSM at the same conditions. This work also discovers that application of H drastically reduces

the thermal conductivity κ , particularly below 4 K, by as much as 40% for both the QSL and HFSM but causes no discernible change in the density of states in the same T range ($1.7 < T < 10$ K). The H-reduced κ is most likely a result of a significantly reduced mobility of spinons as heat carriers. All these complex behaviors suggest an intriguing, simplifying explanation: Application of H adversely weakens the itineracy of spinons and eventually destroy it when T approaches absolute zero, leading to an exotic quantum state featuring the astonishing rise in C, thus entropy at the most unlikely conditions of $T < 150$ mK and $\mu_0 H = 14$ T.

The basic structure of the material is that of a trimer lattice (**Fig.1a**). A trimer unit consists of three face-sharing metal-oxygen (or chalcogen) octahedra. A trimer lattice often behaves unconventionally because its internal degrees of freedom due to delicate couplings between the three metal ions provide an extra, decisive interaction, which, coupled with other fundamental interactions (e.g., Coulomb and spin-orbit-interactions), often dictates physical properties. It has become increasingly clear that heavy transition metal trimer lattices promise a unique pathway to discoveries of new quantum states absent in materials with other types of lattices, such as triangular and perovskite lattices [1, 9-18]. The 4*d*-electron trimer lattice is a perfect example [1].

The trimer lattice adopts a rhombohedral structure with the R-3 space group (No. 148), in which a Nb-O monomer separates trimer layers along the *c* axis (**Fig.1a**) [1, 9, 19]. Depending on Nb concentration, the system exhibits both the HFSM and adjacent QSL phases [1]. The former corresponds to $\text{Ba}_4\text{Nb}_{0.81}\text{Ru}_{3.19}\text{O}_{12}$ or $\text{Nb}_{0.81}$ and the latter $\text{Ba}_4\text{Nb}_{1.16}\text{Ru}_{2.84}\text{O}_{12}$ or $\text{Nb}_{1.16}$ (**Fig.1a**). All other compounds presented in the discussion are specified.

We first focus on the heat capacity C for 50 mK – 1 K at $\mu_0 H = 0$ and 14 T for the two phases (**Fig.1b-c**). As already established in our previous study [1], at $\mu_0 H = 0$ T, a linear C is persistent down to 50 mK with a large Sommerfeld coefficient γ up to 240 mJ/mole K² (**Fig.1b-c**).

However, at $\mu_0 H = 14$ T, C rises rapidly below $T_s = 150$ mK for both the HFSM and QSL (**Fig.1b-c**). The increase in C due to H , defined by $\Delta C/C(0) = [C(H) - C(0)]/C(0)$, can reach as high as 5000% at 50 mK (**Fig.2a-2b**). This H -induced, huge entropy enhancement below T_s strikingly contradicts conventional wisdom that strong H along with low milli-Kelvin T should naturally reduce entropy via reducing disorders and/or degrees of freedom, such as 14 T and 50 mK.

Moreover, sharply contrasting with C (**Fig.1b-c**), both the a -axis resistivity ρ_a for the HFSM and AC magnetic susceptibility χ_a' for the QSL culled in the same T range display a *featureless* response to 14 T (**Fig.2c-2d**).

It is important to be pointed out that ΔC is independent of the orientation of H for both HFSM and QSL. This is evidenced in C as functions of T at $\mu_0 H = 14$ T (**Fig.1b-1c**) and H at $T = 100$ mK (**Fig.2e**). The lack of the orientation dependence indicates an absence of the orbital coupling and an important role of the Zeeman interaction through which the relevant degrees of freedom couple to H , which further highlights the nature of spinons as fractional excitations. In contrast, both ρ_a and ρ_c at higher temperatures for the QSL are a strong function of H -orientation, exhibiting a strong oscillatory behavior with the angle between H and the applied current I (**SFig.1**). The magneto-resistivity ratio, defined by $\Delta\rho/\rho(0) = [\rho(H) - \rho(0)]/\rho(0)$, can be as high as 60% at 9 T. Remarkably, $\Delta\rho/\rho(0)$ is positive for the a -axis ρ_a and negative for the c -axis ρ_c (**SFig.1**). Such a giant, anisotropic oscillatory magnetoresistance suggests an orbital quantum interference in the variable range hopping regime [20 and references therein], which is interesting in its own right (Note no long-range magnetic order down to 50 mK). Nevertheless, the contrasting transport behavior further highlights the spin-charge separation in the system.

For comparison and contrast, C for a related trimer metal $9R\text{-BaRuO}_3$ as well as insulating Nb_2O_5 is also measured as functions of T (**Fig.1d**) and H (**Fig.2f**) at the same experimental

conditions. Both the T- and H-dependences of C exhibit no similarities to those of the HFSM and QSL (**Figs.1b-1c** and **2e**), which decisively eliminates any possible effects from Ba, Ru, and Nb elements that would cause the observed ΔC . Therefore, ΔC must be unique to $\text{Ba}_4\text{Nb}_{1-x}\text{Ru}_{3+x}\text{O}_{12}$.

The H-induced upturn in C (**Fig.1b-c**) could be related to a possible Schottky-like effect due to a splitting of the two-level states, δ , and it could then be a high-T tail of a Schottky peak that might be located well below 50 mK, experimentally inaccessible, but become visible because H broadens δ , which shifts up the Schottky peak to higher T. As such, for $T \gg \delta$, the Schottky contribution to C is expectedly proportional to DT^{-2} (D = Schottky coefficient). Combining DT^{-2} with γT due to spinons yields the total $C = \gamma T + DT^{-2}$ that describes C for both phases for $50 \text{ mK} \leq T \leq 1 \text{ K}$ in the presence of a strong H. Note that the phonon contribution to C is nearly zero in this T range [1]. Fitting $C(T, 14T)$ to $C/T = \gamma + DT^{-3}$ generates a linear fit, yielding slope values of D for both phases at $\mu_0 H = 14 \text{ T}$ (**Fig.3a**). Additionally, $C(H)$ basically scales with H^2 below 200 mK (**Fig.3b**). Here, a few features are remarkable: (1) The D values for both the HFSM and QSL are essentially identical, suggesting that the degrees of freedom responsible for ΔC are the same, and (2) The magnitude of the D values, 10^{-3} JK/mole , is three orders of magnitude greater than that, 10^{-6} JK/mole , due to the quadrupolar and/or magnetic spin splitting of Ru nuclei [21 and references therein], suggesting that the Schottky physics (if such it is) is *not* of nuclear origin. Furthermore, a conventional Schottky peak shifts up sensitively with increasing H that widens the splitting; however, this sensitivity is either weak or absent, as shown in **Fig.3c-3d**. For comparison, similar measurements are conducted for a 2.5% Pr doped isostructural $\text{Ba}_4\text{Nb}_{1-x}\text{Ru}_{3+x}\text{O}_{12}$ i.e., $\text{Ba}_{3.90}\text{Pr}_{0.10}\text{Nb}_{0.84}\text{Ru}_{3.16}\text{O}_{12}$, in which the Pr doping introduces a clear Schottky anomaly characterized by an upturn in C at $H = 0$ below 200 mK (**Fig.3e**). This Schottky anomaly readily shifts to higher T with increasing H, sharply contrasting with that for the HFSM and QSL in **Fig.3c-**

3d, in which the upturn in C is also much more abrupt, compared to that in **Fig.3e**. All in all, the data in **Fig.3** suggest that any arguments based on the conventional Schottky effect alone do not provide an adequate explanation of the H-induced ΔC at $T < T_s = 150$ mK.

We now turn to the thermal conductivity κ for 1.7 K – 10 K at selected H. Our previous study has already established that the QSL is a much better thermal conductor than the HFSM [1]. What is equally intriguing is that application of a magnetic field readily suppresses κ in both phases (**Fig.4a-4b**). This is inconsistent with experimental precedents [e.g., 22, 23, 24, 25, 26]. Generally, κ is proportional to C , the velocity v of heat carriers and the mean free path l of the heat carriers, i.e., $\kappa \sim Cvl$. Because v and l are essentially constant at low T [27], hence C dictates κ . Here, since C does not change with H in the same temperature range, as shown in **Fig.4d-4e**, the significantly reduced κ indicates a significant reduction of the spinon velocity v in the thermal gradient due to H. It cannot be ruled out the shortening of l of the spinons at the same time. As shown in **Fig.4a**, the magnetic field effect on the a -axis κ_a is strong initially when H increases from 0 T to 7 T but becomes weaker as H further increases from 7 T to 14 T, suggesting a trend for saturation with increasing H, which is consistent with the argument.

Furthermore, a close examination of κ at selected H in **Fig.4a-4b** reveals that the magnetic-field effect on κ_a is a strong function of T below 4 K. Here, we introduce a magneto-thermal-conductivity ratio, defined by $\Delta\kappa_a/\kappa_a(0T) = [\kappa_a(14T) - \kappa_a(0T)]/\kappa_a(0T)$, to assess the reduction in κ_a due to the applied 14 T. Note that $\Delta\kappa_a$ reflects contributions from heat carriers that are susceptible to H, or simply H-reduced κ_a . Since the QSL is a charge insulator, $\Delta\kappa_a$ must be due primarily to spinons at low T . As shown in **Fig.4c**, $\Delta\kappa_a/\kappa_a(0T)$ as a function of T shows an unusually large reduction in κ_a . This reduction is considerably stronger in the QSL than in the

HFSM (**Fig.4c**). Such a difference is consistent with there being more spinons as heat carriers in the QSL than in the HFSM (consistent also with the larger C and κ in the QSL [1]), which naturally makes the QSL a much better thermal conductor than the HFSM (**Fig.4a-4b**). Indeed, that $\Delta C/C(0)$ is larger in the QSL than in the HFSM discussed above (**Fig.2a-2b**) provides an additional, key testament to the crucial role of spinons.

In addition, $\Delta\kappa_a/\kappa_a(0T)$ for both phases exhibits a rapid downturn at $T < 4$ K, resulting in a swift reduction in κ_a by as much as 40% near 1.7 K (**Fig.4c**). Because C in the same temperature range remains unchanged (**Fig.4d-4e**), the increasingly negative $\Delta\kappa_a/\kappa_a(0T)$ with decreasing T (**Fig.4c**) forcefully indicates that it must be the mobility of spinons that decreases rapidly with decreasing T as a result of the applied magnetic field. At this rate of the deceleration of spinons, it is entirely conceivable that a strong magnetic field such as 14 T could eventually localize otherwise itinerant spinons when T approaches milli-Kelvin temperatures. This point is schematically illustrated in **Fig.4f**. It is worth mentioning that a study on YbAlO_3 suggests that a staggered molecular field produced by ordered moments confines spinon excitations below the Néel temperature of 0.88 K [28].

Nevertheless, all these phenomena displayed in this work underscore an extraordinary susceptibility of itinerant spinons to applied magnetic fields at milli-Kelvin temperatures, which, however, has never been explored before both experimentally and theoretically.

Here we present and discuss possible explanations. We start by noting that C is independent of H orientation (**Fig.1b-1c**), **Fig.2e**), which strongly indicates that the relevant degrees of freedom that drive ΔC must couple to H only through the Zeeman interaction, and not through the orbital coupling. That is, C below $T_s = 150$ mK is dominated by spinful degrees of freedom which are either immobile or charge neutral (or both) in the presence of H . As already pointed above as well

as in [1], the obvious candidates are charge-neutral spinons to dominate both C and κ in both the HFSM and QSL. Furthermore, the qualitatively similar behavior of C in both phases (**Fig.1b-1c**) indicates nothing special happens to the spinons at the metal-insulator transition, again consistent with [1].

Now, what produces the sudden upturn in C at $T < T_s$ ($= 150$ mK) and $\mu_0 H = 14$ T (**Fig. 1b-1c**)? Prima facie, the $C \propto H^2/T^2$ scaling over the relevant temperature window of 50-200 mK (**Fig.3b**) suggests that the rapid upturn in C might be the high-T tail of a ‘Schottky anomaly’, as mentioned above, wherein the level splitting of the two-level systems in question is proportional to a Zeeman splitting. Moreover, the signal must come from the valence electronic sector – nuclear spins would produce a signal three orders of magnitude too weak (**Fig.3a**) [21 and references therein] whereas ‘core electron states’ can be ruled out by the absence of any corresponding anomaly in BaRuO₃ and Nb₂O₅ (**Figs. 1d, 2f**). That ρ_a for the HFSM as well as χ_a for the QSL at the same conditions exhibits no corresponding anomaly (**Fig.2c-2d**) further suggests that the upturn in C is not associated to any magnetic transition or charge sector transition. Thus, a reasonable working hypothesis is that the sudden upturn in C is due to a novel *spinon Schottky anomaly* affecting charge-neutral spinons which are present (see [1]) in both the QSL and HFSM.

However, this interpretation requires more detailed explanations. For instance (1) The spinons are itinerant, and dominate thermal conductivity in the absence of H [1], how do they form two-level systems and give rise to a Schottky anomaly? (2) Why does the upturn in C only manifest itself at $T < T_s = 150$ mK (**Fig.1b-1c**)? and (3) Why does the presence or absence of the upturn in C essentially depend on the presence or absence of H but less so on the strength of H (which is particular true for the QSL, **Fig.3d**) whereas in a ‘normal’ Schottky system the onset temperature sensitively depends on the strength of H (**Fig.3e**)?

A crucial clue comes from thermal conductivity data, which indicates that the spinon mobility decreases in the presence of H, and this decrease accelerates at $T < 4$ K, giving rise to the increasingly negative $\Delta\kappa_a/\kappa_a(0T)$ (**Fig.4c**). The H-reduced κ_a indicates that the spinons are itinerant in the absence of H, but less so in the presence of H, and may eventually become localized below $T_s = 150$ mK at $\mu_0H = 14$ T. We propose that the upturn in C arises only when spinons are localized, forming two-level systems. Therefore, the onset temperature T_s ($= 150$ mK) marks the onset of localization temperature (or ‘mobility gap’) of the spinon system in the presence of H. This explains the points (1) and (2).

It remains to explain as to why the spinon Schottky anomaly manifests itself only in the presence of H, and yet its onset T_s is less sensitive to the strength of H. This may be explained if we posit that the zero-field spinon system is in the symplectic symmetry class and, being quasi-two dimensional, experiences weak antilocalization [29]. Turning on the magnetic field would then change the symmetry class, destroying weak antilocalization and opening the door to Anderson localization at low T. Once the spinons localize, two-level systems appear. Note that in this scenario the main role of magnetic field is to change the symmetry class and enable localization, so the presence or absence of magnetic field matters, but the strength of magnetic field is less important. Hence, this explanation neatly resolves the point (3). It is also consistent with the H-reduced κ_a at the few Kelvin scale (**Fig. 4**), which is the expected behavior in the weak antilocalization regime [29].

It thus appears that a minimal explanation for all the experimental observations is that C is dominated by spinons. In the absence of H, the spinons are itinerant down to milli-Kelvin temperatures, because of weak antilocalization physics. Application of magnetic field changes the symmetry class, destroying antilocalization, and opening the door to Anderson localization of

spinons below $T_s = 150$ mK, as schematically shown in **Fig.4g**. Once the spinons localize, they form two-level systems, with a Zeeman splitting proportional to H , and this produces a spinon Schottky anomaly in C .

In the above discussion, we have assumed that localized and itinerant spinons cannot co-exist. This is consistent with the usual lore, but recent theoretical investigations [8, 30] have raised an exotic possibility of excitations with ‘fractionalized’ mobility (aka ‘fractons’). One could thus also invoke a more exotic explanation, wherein the specific heat anomaly ΔC comes from immobile but spinful ‘fracton’ excitations, which pair up to form itinerant spinon composites that dominate thermal transport in the absence of magnetic field. The main role of magnetic field in this scenario would be to ‘pull apart’ the mobile spinon composites into the immobile ‘fracton’ excitations. However, it would be necessary to explain as to why the ‘field-induced unbinding’ only happens below the field-independent critical temperature T_s , which does not have an obvious explanation. Therefore, this scenario seems less as natural to us as that of the spinon localization.

In short, the convention-defying behaviors presented here reveal a fundamental relationship between spinons and magnetic fields that has been unexplored until this work: Application of a magnetic field weakens the mobility of spinons and eventually destroys it as temperature approaches absolute zero in a bulk quantum material dictated by spin-charge separation.

METHODS

Single crystals of $\text{Ba}_4\text{Nb}_{1-x}\text{Ru}_{3+x}\text{O}_{12}$ were grown using a flux method. Measurements of crystal structures were performed using a Bruker Quest ECO single-crystal diffractometer with an Oxford Cryosystem providing sample temperature environments ranging from 80 K to 400 K. Chemical analyses of the samples were performed using a combination of a Hitachi MT3030 Plus

scanning electron microscope and an Oxford Energy Dispersive X-Ray Spectrometer (EDX). The measurements of the electrical resistivity, heat capacity, thermal conductivity and AC magnetic susceptibility were carried out using a Quantum Design (QD) Dynacool PPMS system with a 14-Tesla magnet, a dilution refrigerator, a homemade probe for thermal conductivity, and a set of external meters that measure current and voltage with high precision.

DATA AVAILABILITY

The data that support the findings of this work are available from the corresponding authors upon request.

REFERENCES

1. Hengdi Zhao, Yu Zhang, Pedro Schlottmann, Rahul Nandkishore and Gang Cao, Transition between heavy-fermion-strange-metal and spin liquid in a 4d-electron trimer lattice, *Phys. Rev. Lett.* **132**, 226503 (2024)
2. P. W. Anderson, Resonating valence bonds: a new kind of insulator? *Mater. Res. Bull.* **8**, 153–160 (1973)
3. P.W. Anderson, The resonating valence bond state in La_2CuO_4 and superconductivity, *Science* **235**, 1196 (1987)
4. P. A. Lee, An End to the Drought of Quantum Spin Liquids, *Science* **321**, 1306-1307 (2008)
5. L. Savary, L. Balents, Quantum spin liquids: A review, *Rep. Prog. Phys.* **80**, 016502 (2017).
6. Y. Zhou, K. Kanoda, T.-K. Ng, Quantum spin liquid states, *Rev. Mod. Phys.* **89**, 025003 (2017).
7. C. Broholm, R. Cava, S. Kivelson, D. Nocera, M. Norman, T. Senthil, Quantum spin liquids, *Science* **367**, 263 (2020)
8. Rahul M. Nandkishore and Michael Hermele, Fractons, *Annu. Rev. Condens. Matter Phys.* **10**, 295 (2019).

9. L. T. Nguyen, T. Halloran, W. Xie, T. Kong, C. L. Broholm, and R. J. Cava, Geometrically frustrated trimer-based Mott insulator, *Phys. Rev. Mater.* **2**, 054414 (2018)
10. L. T. Nguyen and R. J. Cava, Trimer-based spin liquid candidate $\text{Ba}_4\text{NbIr}_3\text{O}_{12}$, *Phys. Rev. Materials* **3**, 014412 (2019).
11. L. T. Nguyen and R. J. Cava, Hexagonal Perovskites as Quantum Materials, *Chem. Rev.* **121**, 2935 (2021)
12. S. V. Streltsov and D. I. Khomskii, Cluster Magnetism of $\text{Ba}_4\text{NbMn}_3\text{O}_{12}$: Localized Electrons or Molecular Orbitals, *JETP Lett.* **108**, 686 (2018).
13. Evgenia V. Komleva, Daniel I. Khomskii, and Sergey V. Streltsov, Three-site transition-metal clusters: Going from localized electrons to molecular orbitals, *Phys. Rev. B* **102**, 174448 (2020)
14. G. Cao, H. D. Zhao, H. Zheng, Y. F. Ni, Christopher. A. Pocs, Y. Zhang, Feng, Ye, Christina Hoffmann, Xiaoping Wang, Minhyea Lee, Michael Hermele and Itamar Kimchi, Quantum liquid from strange frustration in the trimer magnet $\text{Ba}_4\text{Ir}_3\text{O}_{10}$, *npj Quantum Materials* **5**, 26 (2020)
15. Y. Shen, J. Sears, G. Fabbris, A. Weichselbaum, W. Yin, H. Zhao, D. G. Mazzone, H. Miao, M. H. Upton, D. Casa, R. S. Acevedo-Esteves, C. Nelson, A. M. Barbour, C. Mazzoli, G. Cao, and M. P. M. Dean, Emergence of spinons in layered trimer iridate $\text{Ba}_4\text{Ir}_3\text{O}_{10}$, *Phys. Rev. Lett.* **129**, 207201 (2022)
16. A. Sokolik, S. Hakani, S. Roy Susmita, N. Pellatz, H. Zhao, G. Cao, I. Kimchi, D. Reznik, Spinons and damped phonons in spin-1/2 quantum-liquid $\text{Ba}_4\text{Ir}_3\text{O}_{10}$ observed by Raman scattering, *Phys. Rev. B* **106**, 075108 (2022)

17. Yu Zhang, Yifei Ni, Hengdi Zhao, Sami Hakani, Feng Ye, Lance DeLong, Itamar Kimchi, and Gang Cao, Control of chiral orbital currents in a colossal magnetoresistance material, *Nature* **611**, 467 (2022)
18. Yu Zhang, Yifei Ni, Pedro Schlottmann, Rahul Nandkishore, Lance DeLong and Gang Cao, Current-sensitive Hall effect in a chiral-orbital-current state. *Nat Commun* **15**, 3579 (2024)
19. Supplemental Material, experimental details.
20. L. B. Ioffe, B. Z. Spivak, Giant magnetoresistance in the variable-range hopping regime. *J. Exp. Theor. Phys.* **117**, 551–569 (2013)
21. Z. X. Zhou, S. McCall, C.S. Alexander, J.E. Crow, P. Schlottmann, A. Bianchi, C. Capan, R. Movshovich, K.H. Kim, M. Jaime, and N. Harrison, M. Haas, R. Cava and G. Cao, Transport and thermodynamic properties of $\text{Sr}_3\text{Ru}_2\text{O}_7$ near the quantum critical point, *Phys. Rev. B* **69**, 140409 (2004)
22. Ian A. Leahy, Christopher A. Pocs, Peter E. Siegfried, David Graf, S.-H. Do, Kwang-Yong Choi, B. Normand, and Minhyea Lee, Anomalous Thermal Conductivity and Magnetic Torque Response in the Honeycomb Magnet $\alpha\text{-RuCl}_3$, *Phys. Rev. Lett.* **118**, 187203 (2017)
23. P. Czajka, T. Gao, M. Hirschberger, *et al.* Oscillations of the thermal conductivity in the spin-liquid state of $\alpha\text{-RuCl}_3$. *Nat. Phys.* **17**, 915–919 (2021)
24. J F Gregg and D ter Haar, On the effect of a magnetic field on the thermal conductivity, *Eur. J. Phys.* **17** 303 (1996)
25. Rajasree Das, Amit Chanda and Ramanathan Mahendiran, Influence of magnetic field on electrical and thermal transport in the hole doped ferromagnetic manganite: $\text{La}_{0.9}\text{Na}_{0.1}\text{MnO}_3$, *RSC Adv.* **9**, 1726 (2019)

26. N. Wakeham, A. Bangura, X. Xu, *et al.* Gross violation of the Wiedemann–Franz law in a quasi-one-dimensional conductor. *Nat Commun* **2**, 396 (2011)
27. F. Steckel, A. Matsumoto, T. Takayama, H. Takagi, B. Buchner and C. Hess, Pseudospin transport in the $J_{\text{eff}} = 1/2$ antiferromagnet Sr_2IrO_4 , *EPL* **114** 57007 (2016)
28. L.S. Wu, S.E. Nikitin, Z. Wang, W. Zhu, C.D. Batista, A.M. Tsvelik, A.M. Samarakoon, D.A. Tennant, M. Brando, L. Vasylechko, M. Frontzek, A.T. Savici, G. Sala, G. Ehlers, A. D. Christianson, M.D. Lumsden and A. Podlesnyak, Tomonaga–Luttinger liquid behavior and spinon confinement in YbAlO_3 *Nature Commun* **10**, 698 (2019)
29. S. Hikami, A.I. Larkin and Y. Nagaoka, Spin-orbit interaction and magnetoresistance in the two dimensional random system, *Progress of Theoretical Physics* **63**, 2, 707 (1980)
30. A. Gromov and L. Radzihovsky, *Colloquium: Fracton matter*, *Rev. Mod. Phys.* **96**, 011001 (2024)

ACKNOWLEDGEMENTS G.C. thanks Xi Dai, Tai-Kai Ng, Feng Ye, Sandeep Sharma, Minhya Lee and Longji Cui for useful discussions. Experimental work is supported by National Science Foundation via Grant No. DMR 2204811. Theoretical work by R.N. was supported by the U.S. Department of Energy (DOE), Office of Science, Basic Energy Sciences (BES) under Award # DE-SC0021346.

AUTHOR CONTRIBUTIONS

Y.Z. conducted measurements of the physical properties; H.D.Z characterized the crystal structure of the crystals and conducted measurements of the physical properties. T.R.C. grew the single crystals and conducted measurements of the physical properties. R.N. conducted the theoretical analysis and contributed to paper revisions; G.C. initiated and directed this work, grew the single crystals, analyzed the data, constructed the figures, and wrote the paper.

COMPETING INTERESTS

The authors declare no competing interests.

FIGURE LENGENDS

Fig. 1. Phase diagram and key features. **a**, A schematic phase diagram for the heavy spinon fermi surface featuring the extraordinarily large Sommerfeld coefficient γ (blue) and exchange energy θ_{CW} (red, right scale) as a function of Nb content x for the entire $Ba_4Nb_{1-x}Ru_{3+x}O_{12}$ series [1]. Inset: The crystal structure of the trimer lattice. Note that the heavy-fermion strange metal (HFSM, $1-x = 0.81$ or $Nb_{0.81}$) and the insulating quantum spin liquid (QSL, $1-x = 1.16$ or $Nb_{1.16}$) are adjacent to each other. The heat capacity $C(T)$ for $50 \text{ mK} \leq T \leq 1 \text{ K}$ at magnetic fields $\mu_0 H = 0$ and 14 T for **b**, the HFSM, and **c**, the QSL for both $H \parallel a$ axis and $H \parallel c$ axis. The black arrows mark the onset of the upturn in C . **d**, $C(T)$ for $9R\text{-BaRuO}_3$ and Nb_2O_5 culled at the same conditions for comparison; note that C behaves normally, without any upturn at 14 T observed in the HFSM and QSL.

Fig. 2. Physical properties of the HFSM and QSL. The H -dependence of $[C(H) - C(0)]/C(0)$ at selected T for **a**, the QSL and **b**, the HFSM. The T -dependence for $50 \text{ mK} \leq T \leq 1 \text{ K}$ of **c**, the a -axis ρ_a for HFSM, **d**, the a -axis AC susceptibility χ'_a for the QSL at representative H . The H -dependence at $T = 100 \text{ mK}$ and $\mu_0 H = 14 \text{ T}$ of C for **e**, the QSL for both $H \parallel a$ axis and $H \parallel c$ axis, and **f**, $BaRuO_3$ for $H \parallel c$ axis for comparison. Note $C(H)$ for the QSL is independent of the orientation of H .

Fig. 3. The Schottky-like effect. **a**, C/T vs. $1/T^3$ for $50 \text{ mK} \leq T \leq 1 \text{ K}$ for both the HFSM and QSL. Note the slope D ($\sim 10^{-3} \text{ JK/mole}$) for both phases is essentially the same, and three orders of magnitude larger than that due to the quadrupolar and/or magnetic spin splitting of Ru nuclei. **b**, C as a function of H^2 at representative T for the QLS. $C(T)$ for $50 \text{ mK} \leq T \leq 600 \text{ mK}$ as a function of T at selected H for **c**, the HFSM, **d**, the QLS, and **e**, $Ba_{3.90}Pr_{0.10}Nb_{0.84}Ru_{3.16}O_{12}$ for comparison; the black arrows are a guide to the eye. Note the distinct differences in the sensitivity and the sharpness of the upturn in C between the compounds.

Fig. 4. Thermal conductivity κ at magnetic fields. The T -dependence for $1.7 \text{ T} \leq T \leq 10 \text{ K}$ of the a -axis κ_a at representative H for **a**, the QLS, and **b**, the HFSM. Note the same scale of κ_a in **a**

and **b** and the significant suppression of κ_a due to H. **c**, $\Delta\kappa_a/\kappa_a(0T)$ as a function of T for the QLS and HFSM where $\Delta\kappa_a = \kappa_a(14T) - \kappa_a(0T)$. Note the rapid drop in $\Delta\kappa_a/\kappa_a(0T)$ as $T \rightarrow 0$. **C(T)** for the same T range at $\mu_0H = 0$ and 14 T for **d**, the QSL and **e**, HFSM. Note that **C(T)** remains essentially unchanged at 14 T. **f**, Schematic illustrating the spinons (green dots) as heat carriers at $H = 0$ and $H \neq 0$ and that H reduces the spinon velocity v at $T > T_s$ and destroys it, localizing the spinons at $T < T_s$. **g**, Schematic T-H phase diagram for the spinons at low T.

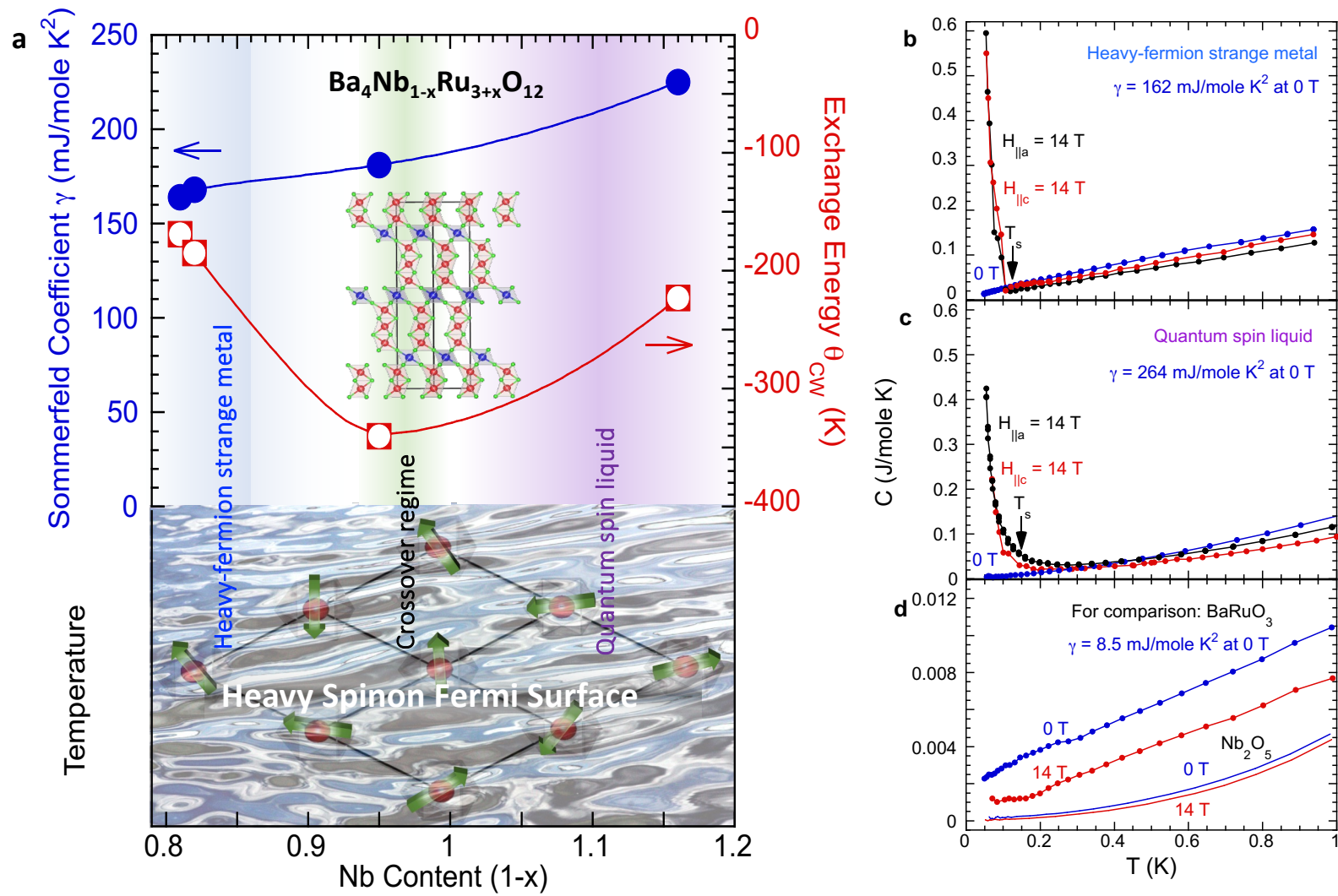


Figure 1

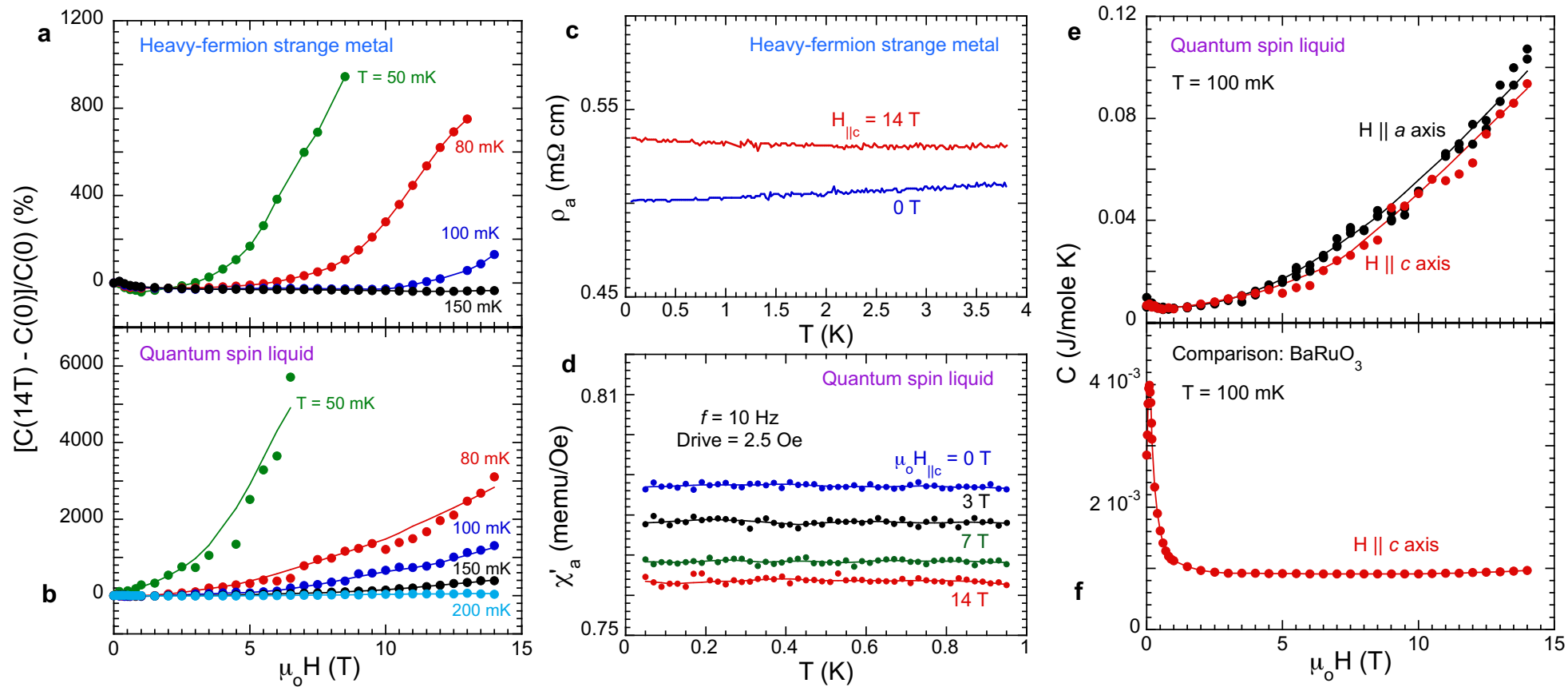


Figure 2

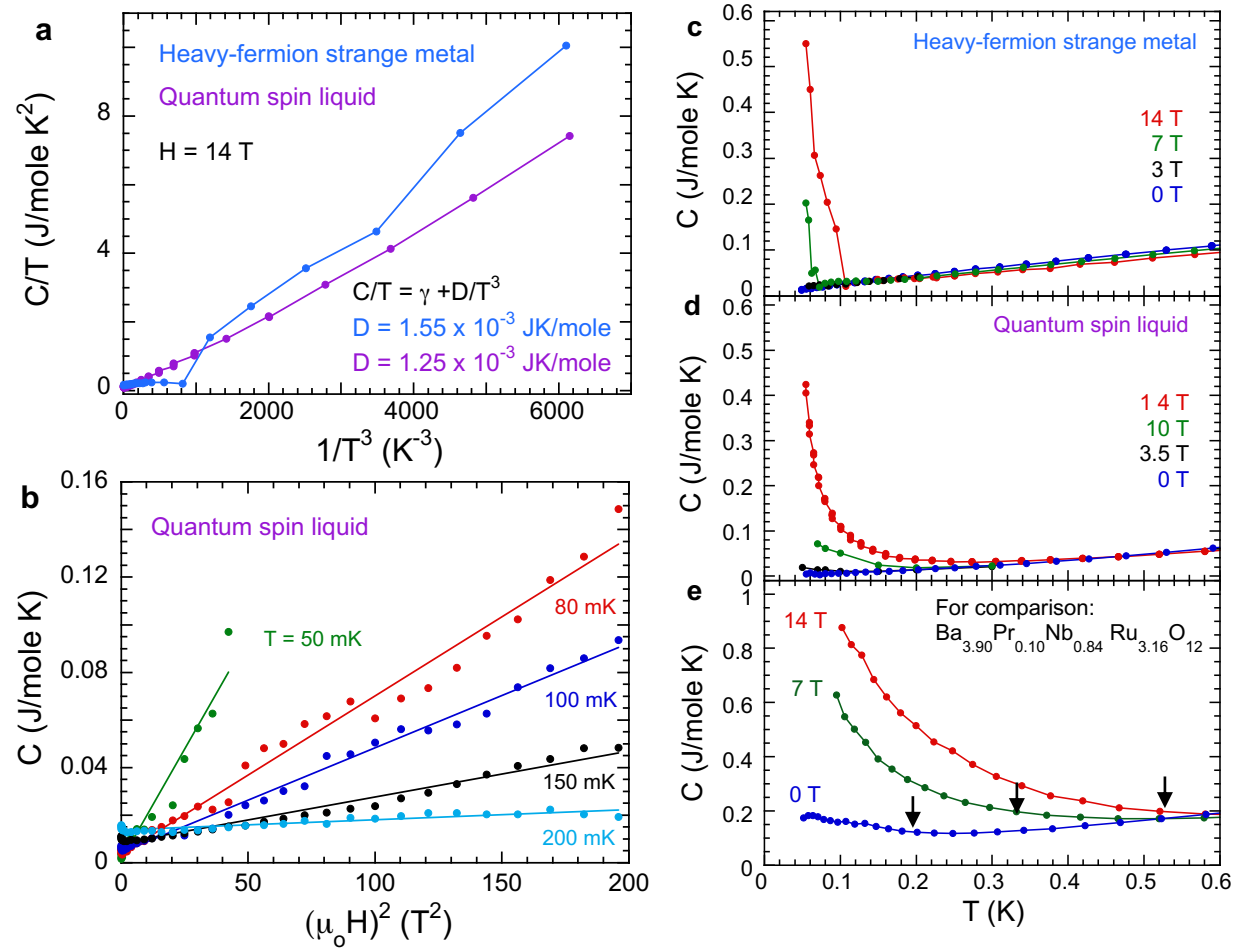


Figure 3

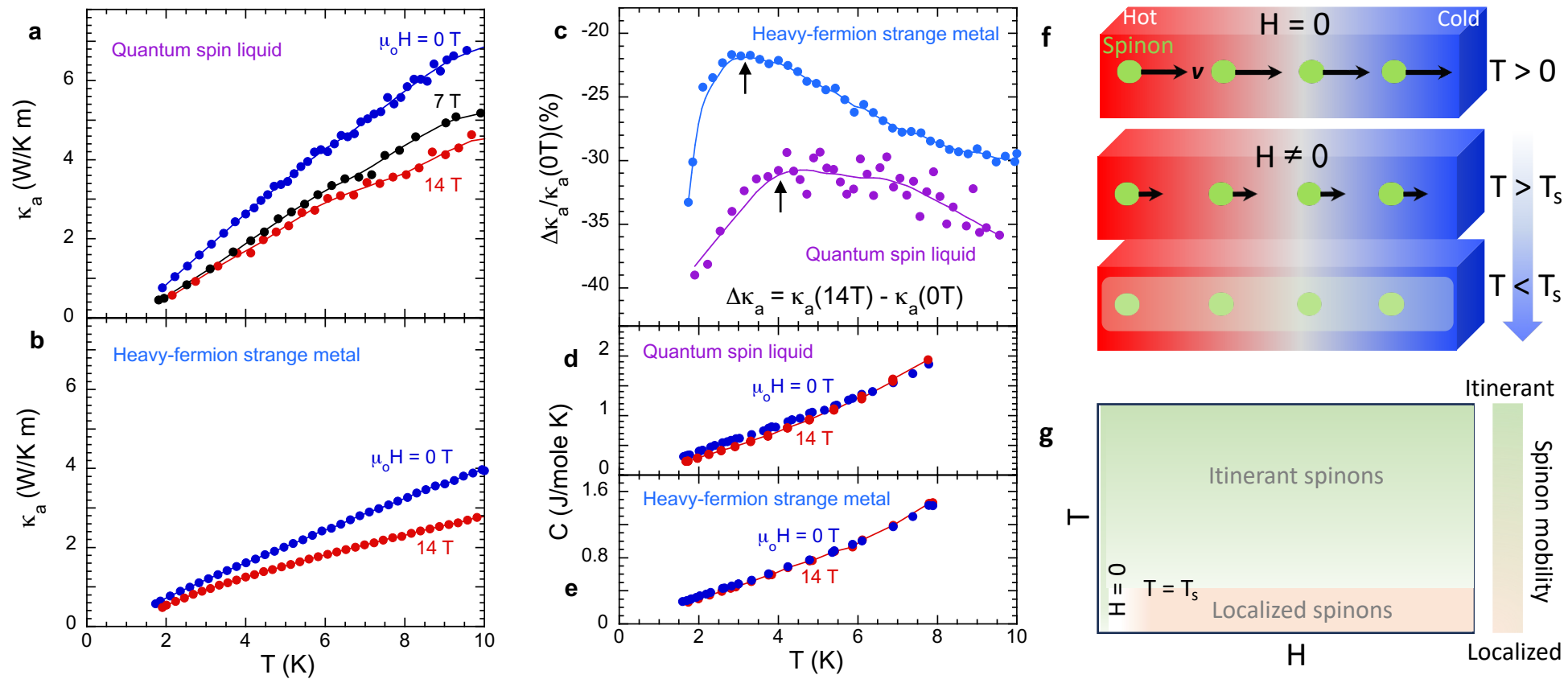


Figure 4